ARTICLES

Quantitative Interpretation of K-Edge NEXAFS Data for Various Nickel Hydroxides and the Charged Nickel Electrode

X. Qian,[†] H. Sambe,[†] D. E. Ramaker,*[,†,‡] K. I. Pandya,[§] and W. E. O'Grady[‡]

Chemistry Department, George Washington University, Washington, DC 20052, Surface Chemistry Branch, Code 6170, Naval Research Laboratory, Washington, DC 20375, and Physics Department, North Carolina State University, Raleigh, North Carolina 27695

Received: February 4, 1997; In Final Form: May 24, 1997[⊗]

A quantitative interpretation of Ni K-edge NEXAFS spectral line shapes for β-Ni(OH)$_2$, β-NiOOH, and $BaNiO_3$ and of in situ data for a charged Ni electrode are reported. We have performed curve−wave multiple scattering calculations utilizing the FEFF6 code on clusters approximating these materials. These theoretical results reproduce the experimental line shape changes with oxidation remarkably well. Our interpretation of the NEXAFS line shape for the charged electrode indicates that large amounts of Ni coordinated with six oxygen atoms exist along with Ni coordinated with two OH and four oxygen atoms, giving an average oxidation state slightly greater than 3.5, consistent with that shown elsewhere from the edge shift data.

1. Introduction

Nickel hydroxides are important materials with applications in nickel batteries,[1] fuel cell electrodes,[2] electrolyzers,[3] and electrochromic devices.[4] As a result, many studies have been reported on these materials, including infrared (IR),[5] Raman,[6,7] X-ray diffraction (XRD),[8] and near-edge[9,10]and extended[11,12,13] X-ray absorption spectroscopy (NEXAFS and EXAFS), as well as several electrochemical studies.[14,15] Despite these many studies, extending over nearly a century, there are still many unanswered questions and controversies concerning these materials. Some of the problems arise because many structural phases exist (e.g., α- and β-Ni(OH)$_2$, and β- and γ-NiOOH) and the dominant phase depends on the method of preparation. Furthermore, the crystallinity of these phases is often inherently poor, and for the charged Ni electrode the data must be collected in situ. Reviews have been published summarizing the extensive literature, the problems, and the questions that remain.[15]

In this work, we will concentrate on the Ni electrode and in particular the oxidation of β-Ni(OH)$_2$ to β-NiOOH or beyond that to a higher oxidation state. The nanostructure of the nickel electrode can be simply described as a layered structure of slabs consisting of three atomic sheets, O−Ni−O. Interspersed between the slabs are "galleries" in which various mobile species may reside.[16] The Ni atoms, lying between the hexagonally close-packed sheets of O, occupy essentially all of the octahedral positions. In the reduced form, β-Ni(OH)$_2$, the gallery is filled with H atoms; i.e., each O atom is bonded to one H atom. Thus β-Ni(OH)$_2$ is generally well-ordered crystallographically within the slabs (although some variation in the registry of the slabs and the widths of the galleries between the slabs can occur), a reasonably good XRD pattern is obtained, and its structure is well-characterized.[8,9,11−13,15]

The oxidation of the Ni electrode involves the removal of H^+ ions from the gallery and transfer into the electrolyte. The extent of this H removal ($^1/_2$ to $^3/_4$ of the total), and the positions occupied by the remaining H atoms are still open to question. Indication exists from XRD and EXAFS data that the remaining H atom distribution is rather disordered: hence the lack of crystallinity even within the O−Ni−O slabs of β-NiOOH or in the fully charged electrode.[8,9,11−13,15] This lack of crystallinity has prevented complete structural characterization with XRD data and in particular prevents knowledge of the location and distribution of the H atoms. Finally $BaNiO_3$ has a rather different structure, with columns of NiO_6 octahedra lined face-to-face, instead of edge-to-edge as in the slabs of Ni(OH)$_2$, giving a well-ordered material and a sharp XRD pattern.[9,17]

The extent of H removal and its distribution in the Ni hydroxides raises many questions in addition to those above. In particular, what factors prevent further H removal from the charged electrode, giving a higher Ni oxidation state? These questions are crucial to the functioning of a battery containing a Ni electrode because if further H atoms could be removed the specific capacity of the battery could be increased. For example, if instead of removing just $^1/_2$ of the H atoms, $^3/_4$ of them could be removed, then the specific energy of the battery could be increased by 50%.

In previous work, the extent of H removal, namely the x value in the chemical formula $NiO_x(OH)_{2-x}$, has been indicated in the context of the formal oxidation state, n, of the Ni atoms.[18] Thus β-Ni(OH)$_2$ has formal oxidation state Ni^{2+} ions, and NiOOH has Ni^{3+} ions where $n = x + 2$. We will comment elsewhere on the actual charge of the Ni atoms present in the various materials, which is very different from the formal oxidation state.[19] Nevertheless, within the present context, if oxidation beyond Ni^{3+} could be achieved, this would suggest the existence of Ni^{4+}. Several papers have previously been published[6,7,9,10,14] asserting evidence for the presence of Ni^{4+}. Perhaps the strongest evidence for this comes from the NEXAFS edge shift.[9,10] In these NEXAFS edge studies, the edge is seen to shift by about 1 eV upward for each increase of 1 in Ni oxidation state, where the edge data for β-Ni(OH)$_2$, β-NiOOH,

* Author to whom correspondence should be addressed.
[†] George Washington University.
[‡] Naval Research Laboratory.
[§] North Carolina State University.
[⊗] Abstract published in *Advance ACS Abstracts,* November 1, 1997.

S1089-5647(97)00435-5 CCC: $14.00

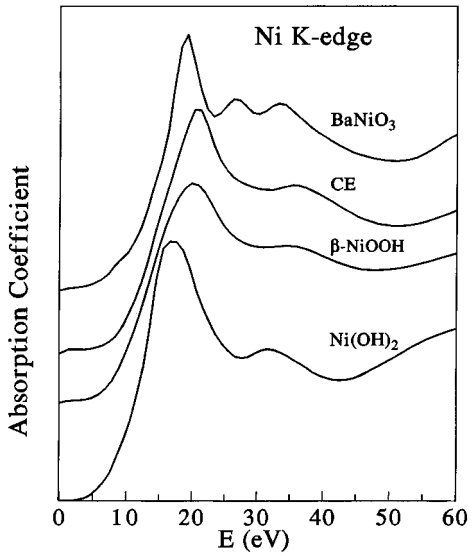

Figure 1. Comparison of the Ni K-edge experimental NEXAFS data (μ) for β-Ni(OH)$_2$, β-NiOOH, $BaNiO_3$, and an in situ charged electrode as previously published by O'Grady et al.[9]

and $BaNiO_3$ (or $KNiIO_6$) were used for the standards of Ni in the 2, 3, and 4 oxidation states, respectively.[9,10] Using this scale, the Ni in the charged Ni electrode was seen to have an oxidation state of 3.5, consistent with previous electrochemical measurements[14] and implying an oxidation value of $x = 1.5$.

Ni K-edge NEXAFS data has previously been published,[9,10] but it was not thoroughly interpreted. In this work we use curved-wave multiple scattering calculations on the appropriate atomic clusters to interpret the NEXAFS spectral line shapes for β-Ni(OH)$_2$, β-NiOOH, $BaNiO_3$, and the charged electrode (CE). We and others have shown that a detailed interpretation of NEXAFS data allows small distortions from octahedral or tetrahedral symmetry to be determined.[20−22] In the Ni hydroxides, these distortions are mainly interpreted as arising from the differences between the Ni−O and Ni−OH bond lengths. Thus the Ni−O bond is elongated to 2.07 Å when a H atom in the gallery is bonded to the O atom, as opposed to 1.88 Å when the O atom is not bonded to a H atom in the gallery. Although EXAFS can provide a measure of the average number of long and short Ni−O bonds as reported[9,11,12] (i.e., the x value in $NiO_x(OH)_{2-x}$), the distribution of these long and short bonds about each Ni atom is not provided by EXAFS. We will provide some qualitative information on these distributions from a detailed interpretation of the NEXAFS data. Furthermore, we will discuss the evidence in the NEXAFS line shape for the presence of Ni^{4+} (i.e., coordinated to six oxygens with no OH) in the charged electrode.

2. Experiment and Theory

The experimental NEXAFS data are taken from O'Grady et al.[9] where the preparation methods for the standard materials are given in detail. X-ray absorption spectroscopy data were obtained for the Ni oxide battery electrodes by recording the data in situ immediately after charging to avoid any possible self-discharge. The experimental details concerning the cell and electrode preparation have been published earlier.[12] Figure 1 shows the experimental data, μ, for the three standard materials and the charged electrode.

Curved-wave, multiple-scattering (CW-MS) cluster calculations utilizing the FEFF6 code developed by Rehr and Albers[23−25] were performed in this work. We have previously[20−22] performed FEFF6 calculations on alkali halides and condensed rare gases (particularly Ne) to test the validity of this code and found that the code reproduces almost all of the experimentally observed peaks except the highly localized excitonic peaks very near or below the edge. For the first-row transition metals and lighter elements, the absolute energy must be shifted by 0−5 eV for optimum agreement with experiment.[20−25] Here, the FEFF6 results were optimally aligned with the experimental data for Ni(OH)$_2$, and then the FEFF6 results for NiOOH and $BaNiO_3$ were shifted by the identical amount.

The input parameters for the theoretical calculations include the atomic number of each unique atom in the cluster, the coordinates of each atom in the cluster, the choice of exchange potential (Hedin−Lundquest, Dirac−Hara, or ground-state), the maximum path length, criteria for the path filter which determines the amount of multiple scattering, the Debye−Waller factor (σ^2), and the charge on the ions. Only positive integers are allowed by the code, so we used zero for the charge in all cases. We have found previously[20−22] that zero charges give the best agreement with experiment even for the case of the alkali halides. Preliminary calculations in the current work for the Ni oxide standards also showed this to be the case. Recent work[19] also shows that the Ni atoms primarily have actual charge of +2 for all oxidation states. We utilized the Hedin−Lundquest potential, which we find, consistent with previous experience,[19−23] gives the best agreement with experiment. The maximum path length was set to 8−10 Å for the one- and two-shell calculations and to 15 Å for the nine-shell calculations. The path filter was chosen to be 1% for the plane waves and 2% for the curved waves (i.e., $^1/_2$ of the default values) to include all important multiple scattering paths. The Debye−Waller factor was set to 0.007.[11,12]

Clusters containing one, two, and nine shells of atoms were used for the calculations. The structures of β-Ni(OH)$_2$ and $BaNiO_3$ are well-known from XRD data[8,17] so that up to nine shells were used for these cases. However, β-NiOOH is not well-ordered, hence the long-range structure is not known; indeed even the Ni coordination is not known. Recent EXAFS results[9] have shown an average of three long (2.07 Å) and three short (1.88 Å) Ni−O bonds about each Ni atom. Therefore FEFF6 calculations were performed on just the one-shell clusters for this case to explore the effects of the bond length and arrangement of the bonds in the octahedral coordination about the Ni atom.

For the one-shell clusters, we utilize a notation $[nl,ns]_{c/t}$ (c = cis; t = trans) that indicates the number of long and short Ni−O bonds about the Ni atom to differentiate the calculations. Recall that long and short Ni−O bonds correspond to OH and O bonds, respectively. It should be noted that two possible arrangements of the [3l,3s] bonds can exist about a Ni atom, namely where three long—or three short—bonds lie in a plane (we call this the "cis" arrangement since the long—or short—bonds are neighboring to each other with C_{3v} symmetry) or where two long and two short bonds are opposite each other (the "trans" arrangement with C_{2v} symmetry). Similarly two arrangements of the [4l,2s] or [2l,4s] exist; namely, where the two long (or 2 short) bonds are opposite (trans with D_{4h} symmetry) or neighboring (cis with C_{2v} symmetry) to each other. We find from the NEXAFS calculations that these cis and trans arrangements introduce relatively small differences (peaks of 5% amplitudes) compared with the 10−20% differences noted in Figure 2 below. Therefore, the larger effects resulting from the number of short bonds (i.e., oxidation) will be examined first, followed by an examination of the smaller effects coming from the cis or trans arrangements of these long and short bonds.

We find it more convenient to compare the differences

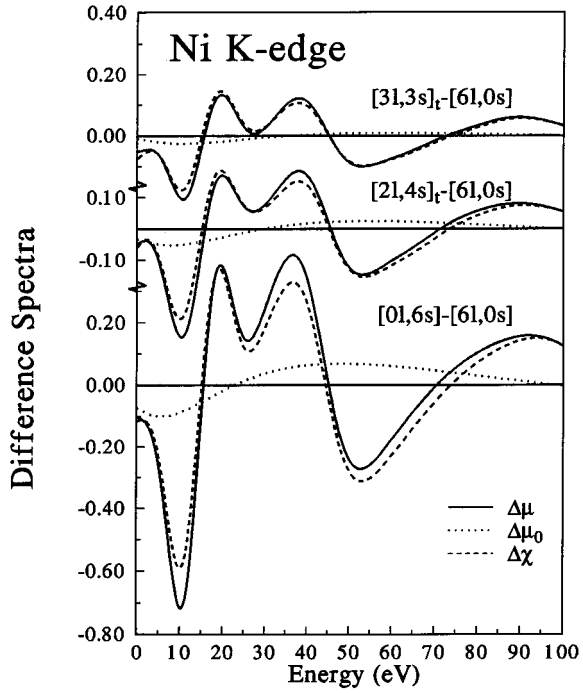

Figure 2. Comparison of FEFF6 results for $\Delta\mu$, $\Delta\mu_o$, and $\Delta\chi$, as defined in the text, for the single-shell calculations $[0l,6s]_t - [6l,0s]_t$. These results show that $\Delta\mu \cong \Delta\chi$.

between μs, that is $\Delta\mu$, for the different Ni hydroxides studied. $\Delta\mu$ emphasizes the small differences seen with oxidation in both the experimental and theoretical NEXAFS spectra. Indeed, the difference spectra reveal features that go completely unnoticed in μ. The absorption coefficient, $\mu = \mu_o(1 + \chi)$, generally has two components, the slowly varying atomic contribution μ_o and the more oscillatory scattering contribution $\mu_o\chi$. Therefore the difference spectra can be approximated as

$$\Delta\mu \equiv \mu - \mu' = \mu_o - \mu_o' + (\mu_o\chi - \mu_o'\chi') \approx \Delta\mu_o + \mu_o\Delta\chi \approx \Delta\chi \quad (1)$$

where $\Delta\mu_o$ is $\mu_o - \mu_o'$ and $\Delta\chi = \chi - \chi'$.

The validity of eq 1 is evident from Figure 2, which shows the relative sizes of $\Delta\mu$, $\Delta\mu_o$, and $\Delta\chi$ for the [*m*l,*n*s]−[6l,0s] (*m* and *n* as indicated) FEFF6 calculations. Generally $\Delta\mu_o$ is a factor of 10 smaller than $\Delta\chi$. Utilizing $\Delta\mu$ also is advantageous since the calculated χ function generally agrees better with the experimental χ than does the calculated μ with the experimental μ. This is because of uncertainties in the calculated μ_o as pointed out by Rehr et al.[23−25] Further, the calculated $\Delta\chi$ agrees better with the experimental $\Delta\chi$ than χ alone. This is because χ has Ni−O antibonding Fano-like resonances which exhibit large multiple scattering contributions not well-represented by the theory.[26] The changes in $\Delta\chi$ can be reasonably well-reproduced with fewer multiple scattering legs as we will discuss further below. Since the overall step heights in the theoretical and experimental μ were normalized to be 1 at an energy well above the edge (100 eV for the theory, 50 eV for the experimental), the amplitudes in the experimental and theoretical difference curves reported in Figures 3−5 are absolute, i.e., indeed $\Delta\mu \approx \Delta\chi$.

The FEFF6 $\Delta\mu$ spectra above 100 eV reveal only very small oscillations about zero (i.e., EXAFS oscillations). The experimental $\Delta\mu$ spectra have had a small straight line background of optimal slope removed to ensure the same behavior, consistent with the usual treatment in EXAFS data analysis.

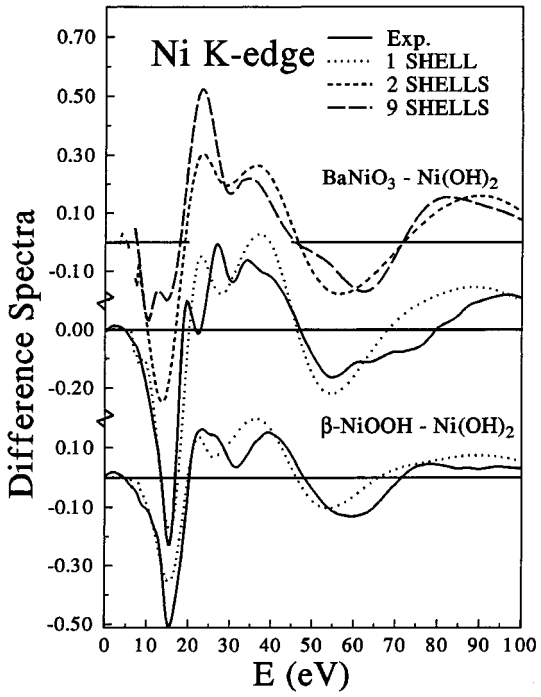

Figure 3. Comparison of experimental difference spectra [$\mu - \mu$(Ni(OH)$_2$] with FEFF6 results on clusters containing one, two, and nine shells approximating β-Ni(OH)$_2$ and $BaNiO_3$. The single-shell calculations are denoted by the notation [0l,6s] − [6l,0s] and $[3l,3s]_t$ − [6l,0s], respectively.

3. Results and Discussion

Figure 3, which compares the experimental and theoretical difference spectra, $\mu - \mu$(Ni(OH)$_2$), for the standard materials, reveals several interesting features:

a. First the magnitude of the negative-going peak around 15 eV indicates the extent of the upward shift of the edge with the oxidation of Ni; thus the negative-going peak is much larger for $BaNiO_3$ than for NiOOH. The relatively good agreement between theory (one-shell calculations) and experiment indicates that indeed the FEFF6 code essentially predicts the relative shifts in the edge with oxidation for the Ni oxides case.[9] Further work is required to determine whether this is generally true.

b. The agreement between theory and experiment for the $BaNiO_3$−Ni(OH)$_2$ is comparable or even better for the one-shell calculations than for the two- and nine-shell calculations. Two questions arise here: (a) why do more shells make the agreement worse? and (b) why is one shell sufficient? A number of possible answers can be given for the first question. First, the nine-shell calculation contains over 100 atoms extending across three O−Ni−O slabs, assuming perfect crystalline order. The worse agreement for the nine-shell calculations may arise from multislab contributions in the theory, which are suppressed in the experimental data because of nonregistry of the slabs, irregularities in the gallery widths, or disorder in the galleries of the Ni(OH)$_2$ material. However, these effects are expected to be small since the Debye−Waller factors should be close to 1 near the edge. Second, it could arise from an underestimate of the imaginary potential near the edge by the Hedin−Lundquest model utilized in these calculations, which would overestimate the contributions from the outer shells. We added a small imaginary potential (0.1 eV) to reduce this problem, but made little effort to optimize the value in this work. Third, as the Ni−O bond gets shorter and stronger (i.e., decreases from Ni(OH)$_2$ to $BaNiO_3$), overlapping muffin-tin spheres may be required to provide better agreement with

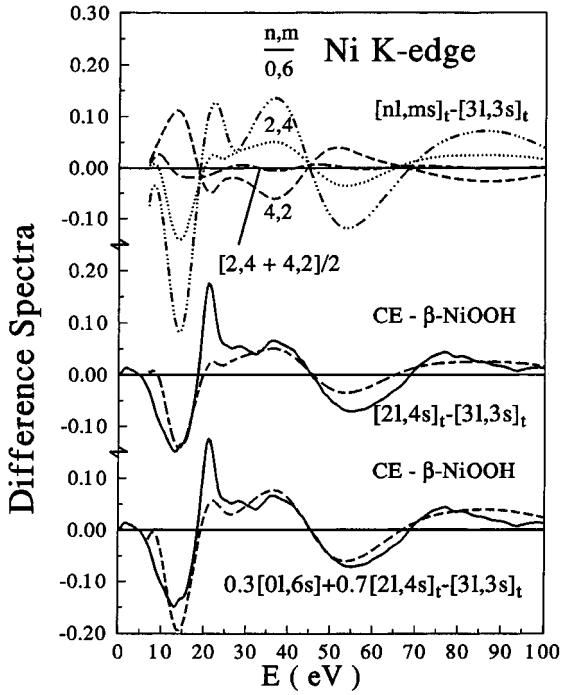

Figure 4. (top) Comparison of $[nl,ns]_t - [3l,3s]_t$ FEFF6 difference spectra showing the increase in amplitude with increasing d_{avg}. (middle) Comparison of experimental difference spectra [μ(CE) − μ(β-NiOOH)] with $[2l,4s]_t - [3l,3s]_t$ FEFF6 results. (bottom) Comparison of μ(CE) − μ(β-NiOOH) with $0.3[0l,6s] + 0.7[2l,4s]_t - [3l,3s]_t$ FEFF6 results.

experiment as found previously by Hudson et al.[27] for uranyl fluoride. One shell is sufficient (question b) because of the effective range of the scattering. It is well-known that heavy atom scattering dominates at higher energies, and light atom scattering dominates at lower energies. Therefore, one would expect Ni−O scattering to dominate below 100 eV, the region we examine in this work. Even at 100 eV, FEFF6 results showthat Ni−O scattering is 1.5 times Ni−Ni scattering. Furthermore, the higher shell Ni−O scattering is small as revealed by the previously published[9,10] Fourier transforms of χ.

c. The agreement between the theory and experiment for the one-shell calculations is remarkable considering that the average magnitude of the differences in the data amount to around 10−20% of the total absorption coefficient as shown in Figure 1.

d. A feature growing in intensity around 25 eV with oxidation is known to arise from a many-body charge-transfer shake-up excitation and, therefore, is not reproduced by the FEFF6 calculations.[28]

In light of the excellent agreement between the single-shell FEFF6 results and the experimental results obtained for the standard materials in Figure 3, we proceed to compare results for the charged electrode (CE) with β-NiOOH; i.e., we examine μ(CE) − μ(β-NiOOH). This suggests comparison of various $[nl,ms]_t$ and $[3l,3s]_t$ single-shell calculations, since we have shown in Figure 3 that the $[3l,3s]_t$ FEFF6 line shape approximates the NiOOH experimental line shape. Figure 4 compares several single-shell FEFF6 calculations to determine the effect of the *number* of short vs long bonds (i.e., Ni oxidation state) and the *uniformity* of their distribution. These calculations clearly show a strong increase in the amplitude of the oscillations with decreasing average bond length, d_{avg} (i.e., increasing Ni oxidation), but the wavelength (or the nodal positions) of the oscillations is independent of d_{avg}. We derive an analytical expression elsewhere[29] showing that indeed $\Delta\chi$ is proportional to the change in the phase and amplitude (i.e., here primarily coming from, respectively, a change in the Ni−O bond distance and a possible change in the Debye−Waller factor). The difference spectra $([2l,4s]_t + [4l,2s]_t)/2 - [3l,3s]_t$, which compares configurations having the same d_{avg} and bond arrangement (i.e., trans in all cases) but with nonuniform distribution has very small amplitude (less than 2%). Unfortunately, this means that we can shed little light on the uniformity of the H atom distribution; however, the amplitude of the difference spectra gives a good measure of d_{avg}, or the average Ni oxidation.

Figure 4 also shows a comparison between the experimental spectra μ(CE) − μ(NiOOH) with the appropriate FEFF6 calculations on single-shell NiO_6 clusters. On the basis of the examination of the $[nl,ms]_t$ results above, we conclude that the experimental line shape should be reasonably well-approximated by the $[2l,4s]_t - [3l,3s]_t$ FEFF6 line shape. This then provides evidence that the charged electrode is oxidized beyond that in NiOOH (Ni^{3+}, $x = 1$); namely containing some $NiOOH_{0.67}$ (i.e., $Ni^{3.3+}$, $x = {}^4/_3$) consistent with the [2l,4s] configuration.

Although reasonable agreement in the line shapes exist between the $[2l,4s]_t - [3l,3s]_t$ FEFF6 line shape and the experimental difference spectra, the amplitude of the oscillations in the $[2l,4s]_t - [3l,3s]_t$ theory are smaller than in the experimental line shape, particularly for $E > 20$ eV where the theory is the most reliable. We emphasize again that the amplitudes in Figure 4 are absolute (note that they are smaller here than in Figure 3 because we are comparing here the CE amplitude with that of β-NiOOH, which are more similar than those of β-$Ni(OH)_2$ and β-NiOOH compared in Figure 3). Since the amplitudes are rather strongly dependent on d_{avg}, this indicates that indeed some Ni with six short bonds (i.e., Ni^{4+}) exist in the charged electrode. This is consistent with the NEXAFS edge data previously reported.[9]

If the average oxidation state is indeed 3.5 (or $x = 1.5$) in the charged electrode and this contains a mix of [2l,4s] and [0l,6s], we would expect the line shape to be represented by $0.7[2l,4s]_t + 0.3[0l,6s]_t$. In Figure 4, we compare this with the experimental difference line shape. The agreement is substantially improved by adding in the $[0l,6s] - [3l,3s]_t$ line shape, confirming the presence of [0l,6s] and that the average oxidation level is of the order of 3.5 or $x = 1.5$.

It is perhaps rather surprising that the amplitudes in the theory are too small since only small Debye−Waller factors having a near negligible effect were included and larger ones to reflect the possible disorder in the charged electrode would make the oscillations in the theory even smaller. If the Debye−Waller factors were increased, even larger amounts of [0l,6s] Ni would be indicated. This suggests that in the charged electrode the H atom distribution is well-ordered, much more than in β-NiOOH.

Figure 5 examines the effect of the *arrangement* (cis or trans) of the long and short bonds about a Ni atom. Since we do not know the preferred arrangement in either the β-NiOOH or the charged electrode, we have four possible combinations (c−t, c−c, t−c, t−t). First we compare the FEFF6 results for the four combinations in the difference spectra. Note that the c−t and t−c combinations are the most different in the region between 15 and 28 eV, with the c−c and t−t combinations reflecting some average of these first two. This is the reason we utilized the t−t combination in Figures 3 and 4. Figure 5 now compares the optimal fit of $x[0l,6s] + (1 - x)[2l,4s]_{c/t} - [3l,3s]_{c/t}$ for the four combinations and compares the R factor for these combinations. Here we used the R factor, $R = \sum(\text{theor} - \text{expt})^2/[\sum(\text{theor})^2 + \sum(\text{expt})^2]$, which equals 0 for a perfect fit, 1 if theory and experiment are uncorrelated, and 2

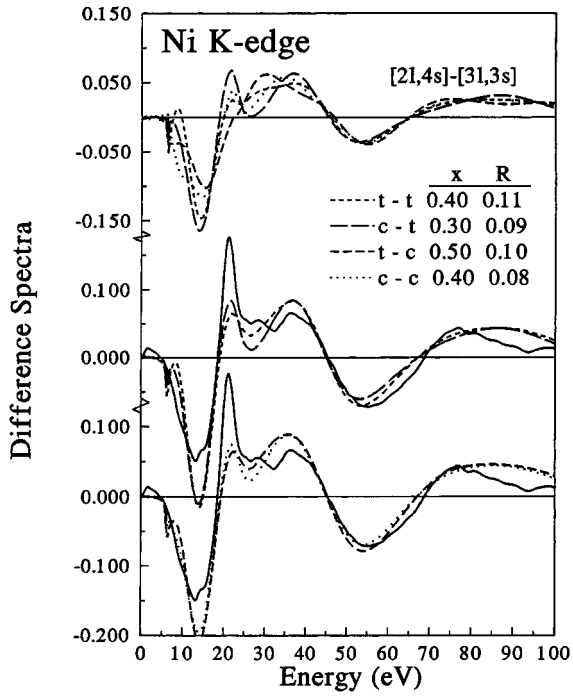

Figure 5. (top) Comparison of the $[2l,4s]_{c/t} - [3l,3s]_{c/t}$ FEFF6 results for the four possible cis/trans arrangements (c−c, c−t, t−c, and t−t) of the long and short Ni−O bonds about a single Ni atom. (bottom) Comparison of the least-squares fit of $x[0l,6s] + (1 - x)[2l,4s]_{c/t} - [3l,3s]_{c/t}$ to the experimental results, μ(CE) − μ(β-NiOOH) (solid line), for the four cis/trans combinations. The ledger shows the optimum value of x and the R factor as defined in the text for each combination.

if they are anticorrelated (summation signs indicate sums over the number of points).[30] Although the c−c combination gives the smallest R factor, it is not appreciatively better than the other combinations, so unfortunately these results are inconclusive. Nevertheless, all four optimal fits show that the [0l,6s] contribution is in the range of 30−50% with an average of around 40% consistent with a Ni oxidation of 3.6 or $x = 1.6$ as indicated above.

The arrangement of the long and short bonds (i.e., cis or trans as discussed above) produces only an approximate 4−5% effect on the difference spectra in the Ni oxide as shown in Figure 5. As a result, only qualitative information on the H ordering in the gallery is possible at best. In previous calculations we have performed on $Zn(OH)_4$ and AlO_n ($n = 4$, 5, or 6), distortions from tetrahedral and octahedral symmetry were clearly revealed.[27] Two reasons can be given for this different situation. First, three different rearrangements may alter the line shape, namely changes in the average bond length, bond arrangement, and orthogonality of the bond axes. Here for the Ni hydroxides the average bond length has the largest effect, thus somewhat masking the dependence on the arrangement and orthogonality. Second, the geometric distortions in $Zn(OH)_4$ and AlO_n involved changes of the angle subtended by the "ligand" atoms (i.e., 90° in the octahedral vs 109° in the tetrahedral with a near 10% change in angle), while here we are attempting to determine the bond length arrangement. Hudson et al.[25] have recently shown that multiple scattering "resonances" can arise within collinear short O−M−O axial bonds. These resonant features apparently dissipate rapidly upon removal of the collinear bonding (i.e., angle distortion). Thus, the NEXAFS spectra can be somewhat more sensitive to angle distortions than to bond length arrangement. The FEFF6 calculations that we have carried out confirm this. A 10% distortion in collinear arrangement ($[6l,0s]_{distorted} - [6l,0s]$) produces amplitude changes of magnitude 15%, compared with 4−5% resulting from the c/t bond arrangement ($[2l,4s]_t - [2l,4s]_c$). However, in the Ni compounds studied here, we do not believe that the collinear character of the O−Ni−O bonds is disturbed, because this would require a significant rearrangement of the lattice. Nonorthogonality of the collinear axes may arise, but the affects of these distortions are expected to be even smaller than the bond arrangement effects, so they are completely ignored in this work. Unfortunately, not even the bond arrangement (i.e., H arrangement), an effect expected to be larger than axis nonorthogonality, could be determined here.

Finally, we note that the differences between the optimum theoretical fit and the experimental line shapes around 20−30 eV for the charged electrode in Figure 5 are very similar to those found for $BaNiO_3$ in Figure 3. We believe these differences arises from the charge-transfer satellite present around 27 eV and the effect of this satellite on the line shape throughout the 20−30 eV region. Indeed, in Figures 4 and 5, the small feature around 27 eV reflects the increased satellite in the charged electrode compared with β-NiOOH, giving further evidence that the charged electrode is in a higher oxidation state than β-NiOOH.

4. Summary

A quantitative interpretation of Ni K-edge NEXAFS spectral line shapes for various Ni hydroxides utilizing the FEFF6 code reveals the following: (a) The FEFF6 code can reproduce the line shape changes with oxidation remarkably well. (b) The intensity of the charge-transfer shake-up peak increases with oxidation. This many-body satellite, not reproduced by the calculations, decreases the quality of the agreement with experiment in the 20−30 eV region. (c) FEFF6 calculations indicate that the amplitude of the oscillations in the difference spectra is directly proportional to the average Ni−O bond length and hence directly reflects the average oxidation state of the Ni atom. (d) The difference spectra, relatively insensitive to the cis/trans arrangement of the short and long bonds about a Ni atom, provide only qualitative and tentative information on the ordering and arrangement of the H atoms in the galleries of these Ni materials. (e) The NEXAFS line shape indicates that some Ni with [0l,6s] coordination exists along with Ni having [2l,4s] coordination in the charged electrode, giving an average Ni oxidation state slightly greater than 3.5, consistent with that shown previously from the edge shift.

Acknowledgment. Support from the Office of Naval Research is gratefully acknowledged. The authors also gratefully acknowledge the support of the U.S. Department of Energy, Division of Materials Science, under Contract no. DE-FG05-89ER45384, for its role in development and operation of beam line X11A at the National Synchrotron Light Source (NSLS). The NSLS is supported by the Department of Energy, Division of Material Sciences, under Contract no. DE-AC02-76CH00016. We thank D. Corrigan for helpful discussions.

References and Notes

(1) Oliva, P.; Leonardi, J.; Laurent, J. F.; Demas, E.; Braconis, J. J.; Figlanz, M.; Fievet, F.; Deguibert, A. J. *Power Sources* **1982**, *8*, 229.
(2) Bacon, F. T. *J. Electrochem. Soc.* **1979**, *126*, 7C.
(3) Hall, D. E. *J. Electrochem. Soc.* **1983**, *130*, 317.
(4) Carpenter, M. K.; Conell, R. S.; Corrigan, D. A. *Solar Energy Mater.* **1987**, 16, 333.
(5) Jackovitz, J. F. In *The Nickel Electrode*; Gunther R. G., Gross, S., Eds.; The Electrochemical Society Softbound Processing Series: Pennington, NJ, 1982; PV 82-84, p 48.
(6) Desilvestro, J.; Corrigan, D. A.; Weaver, M. J. *J. Electrochem. Soc.* **1988**, *135*, 885.
(7) Melendres C. A.; Paden, W.; Tani, B.; Walczak, W. *J. Electrochem. Soc.* **1987**, *134*, 762.

(8) Greaves, C.; Thomas, M. A.; Turner, M. in *Power Sources 9*; Thompson, J., Ed.; Acad. Press: New York, 1983.

(9) O'Grady, W. E.; Pandya, K. I.; Swider, K. E.; Corrigan, D. A. *J. Electrochem. Soc.* **1996**, *143*, 1613.

(10) Mansour, A. N.; Melendres, C. A.; Pankuch, M.; Brizzolara, R. A. *J. Electrochem. Soc.* **1994**, *141*, L69.

(11) Pandya, K. I.; O'Grady, W. E.; Corrigan, D. A.; McBreen, J.; Hoffman, R. W. *J. Phys. Chem.* **1990**, *94*, 21.

(12) Pandya, K. I.; Hoffman, R. W.; McBreen, J.; O'Grady, W. E. *J. Electrochem. Soc.* **1990**, *137*, 383.

(13) McBreen, J.; O'Grady, W. E.; Tourillon, G.; Dartyge, E.; Fontaine, A.; Pandya, K. I. *J. Phys. Chem.* **1989**, *993*, 6308.

(14) Corrigan, D. A.; Knight, S. L. *J. Electrochem. Soc.* **1989**, *136*, 613.

(15) McBreen, J. In *Modern Aspects of Electrochemistry*; White, R. E., Bockris, J. O'M., Conway, B. E., Eds.; Plenum Press: New York, 1990; Vol. 21, p 29.

(16) Huggins, R. A.; Prinz, H.; Wohlfahrt-Mehrens, M.; Jorissen, L.; Witschel, W. *Solid State Ionics* **1994**, *70/71*, 417.

(17) Takeda, Y.; Kanamaran, F.; Koizumi, M. *Acta Crystallogr.* **1976**, *B32*, 2464.

(18) The formal oxidation state is defined as that charge which would exist on the metal atom if all ligands were removed to infinity with their shells full; see: Hegedus, L. S. *Transmission Metals in the Synthesis of Complex Organic Molecules*; University Science Books: New York, 1994; pp 1−14.

(19) Sambe, H.; Nabi, T.; Qian, X.; Ramaker, D. E.; O'Grady, W. E.; Mansour, A. N. Unpublished results.

(20) Qian, X.; Sambe, H.; Ramaker, D. E. *Phys. Rev. B* **1995**, *52*, 15115.

(21) Ramaker, D. E.; Sambe, H.; Qian, X.; O'Grady, W. E. *Physica B* **1995**, *208/209*, 49.

(22) Sambe, H.; Qian, X.; Ramaker, D. E. *Phys. Rev. B* **1996**, *53*, 1779.

(23) Rehr, J. J.; Albers, R. C. Phys. Rev. **1990**, *B41*, 8139.

(24) Rehr, J. J.; Zabinsky, S. I.; Ankudinov, A.; Albers, R. C. *Physica B* **1995**, *208/209*, 23.

(25) Zabinsky, S. I.; Rehr, J. J.; Ankudinov, A.; Albers, R. C.; Eller, M. *J. Phys. Rev. B* **1996**, *52*, 2995.

(26) Rehr, J. J.; Albers, R. C.; Zabinsky, S. I. *Phys. Rev. Lett.* **1992**, *69*, 3397.

(27) Hudson, E. A.; Rehr, J. J.; Bucher, J. J. *Phys. Rev.* **1995**, *B52*, 13815; Hudson, E. A., Allen, P. G., Terminello, L. J., Denecke, M. A.; Reich, T. *Phys. Rev. B* **1996**, *54*, 156.

(28) Rehr, J. J.; Stern, E. A. *Phys. Rev. Lett.* **1982**, *49*, 1353. Rehr, J. J.; Stern, E. A.; Martin, R. L.; Davidson, E. R. *Phys. Rev.* **1978**, *B17*, 560.

(29) Ramaker, D. E.; Sambe, H.; Qian, X.; O'Grady, W. E. *J. Phys. IV (France)* **1997**, *7*, C2−233. van Bokhoven, J. A.; Sambe, H.; Koningsberger, D. C.; Ramaker, D. E. *J. Phys. IV (France)* **1997**, *7*, C2−835.

(30) Woodruff, D.; Delchar, T. *Modern Techniques of Surface Science*; Cambridge University Press: New York, 1986; p 67.